Electron-mediated ferromagnetism in Fe-doped InP: Theory and experiment*

Dong Shan(董 珊)† and Zhu Feng(朱 峰)

State Key Laboratory for Superlattices and Microstructures, Institute of Semiconductors, Chinese Academy of Sciences, Beijing 100083, *China*

(Received 13 January 2012; revised manuscript received 11 March 2012)

We report on the electron-mediated ferromagnetism in Fe-doped InP from both first-principles calculations and experiments. Theoretically, based on spin-polarized density functional theory within Heyd–Scuseria–Ernzerhof (HSE03) approach, we systematically investigate the magnetic properties of Fe-doped InP and predict the existence of electron-mediated ferromagnetism. Experimentally, by diffusing Fe into the n-type InP wafer with thermal annealing at 800 °C, we observe room-temperature ferromagnetism in InP:Fe, which is in agreement with the theoretical prediction.

Keywords: ferromagnetism, Fe-doped InP, first-principles calculations

PACS: 75.50.Pp, 71.55.–i, 71.70.–d **DOI:** 10.1088/1674-1056/21/9/097502

1. Introduction

Dilute magnetic semiconductors (DMSs) as a significant foundation for potential spintronic applications are of wide technological interest and importance in basic scientific researches.[1−3] Generally, DMSs obtained by the incorporation of 3d transition-metal (TM) into conversional semiconductor hosts, especially III–V and II–VI semiconductors like GaN and ZnO, show a lot of desirable semiconductor and magnetic properties.[4−8] In particular, ferromagnetic (FM) DMSs with Curie temperature (T_C) exceeding room temperature are required in various spin-dependent devices. Therefore, the fabrication of ferromagnetic semiconductor with high T_C has spawned a large number of studies on TM-doped semiconductors. In the previous studies, several microscopical models have been proposed to depict the spin-coupling mechanism between TM and hosts,[9−11] such as p–d exchange, d–d double-exchange, and superexchange models. These exchange interactions have been widely and successfully used to explain the magnetic ordering observed in TM-doped III–V and II–VI semiconductors. In light of these models, the FM stability crucially depends on the existence of holes localized in d state of TM ions,[12−15] namely, the so-called hole-mediated ferromagnetism. Recently, Walsh *et al.*[16] have achieved the stable FM ground state in Co doped ZnO through n-type doping based on the band coupling model. This is considered as another effective approach to acquiring the high T_C DMSs.

Fe-doped III–V or II–V semiconductors as the basis for various high speed electronic and optoelectronic devices have great potential applications.[17,18] Zhu *et al.*[19] have observed room-temperature spin injection from Fe into GaAs. Feng *et al.*[20] have observed room-temperature ferromagnetism in ZnFeO thin film. Twardowski *et al.*[21] have reported on the values of specific heat and low field susceptibility of $Zn_xFe_{1-x}S$ ($x < 0.26$). However, the values of their Curie temperature T_C are very low (below 20 K). Up to date, few theoretical or experimental investigations of high temperature ferromagnetism in Fe-doped InP have been reported.

In the present work, first of all, we perform an extensive analysis of electron-mediated magnetic properties of Fe-doped InP using first-principles method based on spin-polarized density functional theory (DFT).[22] We find the generalized-gradient approximation (GGA) within the exchange-correlation functional in the form of Perdew–Burke–Ernzerhof (PBE) calculations suppresses the contribution of carrier electrons to the stability of FM magnetic ordering due to the well-known error of underestimating the band gap.[23,24] To reduce this error and predict the correct electron-mediated magnetic ordering, we also carry out the DFT calculations within Heyd–Scuseria–

*Project supported by the National Natural Science Foundation of China (Grant No. 60925016).

†Corresponding author. E-mail: dongshan08@semi.ac.cn

© 2012 Chinese Physical Society and IOP Publishing Ltd

Ernzerhof (HSE03) approach for exact prediction of electronic structure and magnetic properties of Fe-doped InP.[25−28] The results indicate that the carrier electrons can stabilize the FM ordering in terms of the band coupling model. Finally, in order to verify the theoretic prediction of electron-mediated FM ordering, we prepare the InP:Fe wafer by using n-type bulk InP grown by vapour diffusion method as substrate. As expected, this n-type Fe-doped InP wafer shows ferromagnetism at room temperature.

The rest of the present paper is organized as follows. In Section 2 we describe the calculation details and the experimental methods. In Section 3, we present band coupling models to demonstrate the FM and anti-ferromegnic (AFM) ordering of Fe-doped InP bulk materials. The HSE03 calculations predict FM coupling in InP:Fe system. The experimental results of room-temperature ferromagnetism in Fe-doped InP wafers are also presented in Section 3. Finally, some conclusions are drawn from the present study in Section 4.

2. Methods of calculation and experiments

All calculations are performed using first-principles method based on spin-polarized DFT within PBE and HSE03 approaches as implemented by Vienna *ab initio* simulation package (VASP).[29] A 64-atom zinc-blende (ZB) supercell is used in our calculations. To determine the stability of FM or AFM ordering, in the supercell two nearest-neighbours In atoms are replaced by Fe atoms. Convergence with respect to the plane-wave cutoff energy has been checked. The Monkhorst–Pack method is used to sample k-point mesh in the Brillouin zone.[30] A 2×2×2 grid is used in PBE calculations while the Γ point is used in HSE03 calculations. All the structures are allowed to relax until the Hellmann–Feynman force is less than 0.05 eV/Å. For the primitive unit cell, the PBE and HSE03 optimized lattice constants are 5.994 and 5.955 Å, respectively, in good agreement with those given in Ref. [13]. The PBE gives an InP band gap of only 0.84 eV, while the HSE03 gives that of 1.42 eV, which is in good agreement with the experimental value of 1.46 eV given in Ref. [31]. This indicates that the use of HSE03 is more reasonable for predicting InP band structures.

The samples used in the experiments are prepared by Fe-doped InP wafers grown by liquid encapsulated Czochralski (LEC) method in our laboratory. Fe thin films each with a thickness of about 800 nm are deposited by vacuum evaporation at a vacuum level of 10^{-3} Pa. The quantity of Fe power is 6 N. Then we put the InP sample deposited with Fe thin film into a quartz tube at a base pressure of 2×10^{-3} Pa. The annealing is carried out in the sealed quartz tube at 800 °C for 24 h. After annealing, the wafers are cooled at room temperature for about 45 h. Structural characterizations of the samples are carried out by X-ray diffraction (XRD). The compositional properties are monitored by energy dispersive X-ray (EDX). The XRD measurements are performed in Bragg–Brentano geometry. Magnetization measurements are carried out using a superconducting quantum interface device (SQUID) magneto-meter under the magnetic field intensity $\boldsymbol{H}$ perpendicular to the film plane.

3. Results and discussion

The ZB InP belongs to space group $F\bar{4}3m$ with T_d symmetry. As a result, the Fe-3d states split into lower doublet e and upper triplet t_2 states in the tetrahedral ligand field. Moreover, The Fe has d^6s^2 valence electron configuration and becomes Fe^{3+} in InP. Therefore, taking exchange interaction into account, it leads to the full occupation of all the majority spin states and empty occupation of minority spin states. Figure 1 shows the calculated total and local densities of states (DOSs) for Fe e and t_2 states, respectively. It clearly represents that the spin-up t_2 and e states are under the Fermi level, while the spin-down states are above the Fermi level, thereby resulting in a magnetic moment in Fe-doped bulk InP. In terms of d band coupling model, FM repulsion between the spin-up or the spin-down Fe d states results in no net energy gain because of the filled or unfilled bonding or antibonding states (Fig. 2(a)). Here, we assume that the couplings between the two spin-up d levels and the two spin-down d levels lead to splitting of $2\Delta^1_{\rm dd}$ and $2\Delta^2_{\rm dd}$ (as shown in Fig. 2), respectively. However the energy gain of $-3\Delta^{\rm t1,2}_{\rm dd}$–$2\Delta^{\rm e1,2}_{\rm dd}$ is induced in AFM configuration resulting from superexchange repulsion between the filled and unfilled t_2 and e states (Fig. 2(b)). Therefore, the magnetic ground state is AFM. Indeed, the more directly calculated total energy differences between FM and AFM configurations in Fe-doped InP as shown in Fig. 2 are consistent with these expected analysis when there is no additional carrier electron in trapped d level of Fe ion. Usually,

the coupling between t_2 states is much stronger than that between e states due to the strong localization of e state in ZB phase. Therefore, the t_2–t_2 coupling dominates the magnetic ordering.

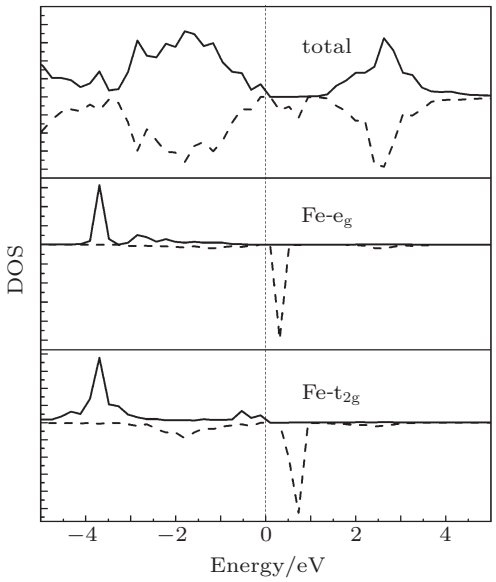


Fig. 1. Calculated total and local densities of states for Fe e and t_2 states, respectively. The Fermi level is indicated by the dashed vertical line. Solid curves are spin-up (majority) bands and dashed curves are spin-down (minority) bands.

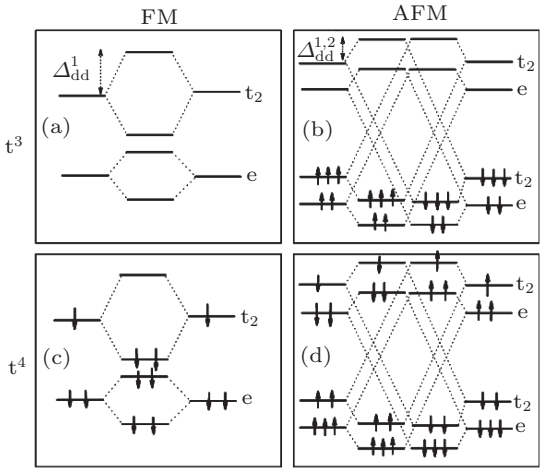


Fig. 2. Schematic band coupling models of Fe t and e levels in FM and AFM configurations. The couplings between the two spin-up d levels and the two spin-down d levels lead to splittings $2\Delta^1_{dd}$ and $2\Delta^2_{dd}$, respectively.

In terms of band couplings, theoretically partial filling of the nominally empty minor Fe t_2 state is expected to stabilize the system into FM from AFM ordering. The corresponding schematic coupling models of FM and AFM are shown in Figs. 2(c) and 2(d). In the FM configuration and spin-up channel, the system does not gain energy through the direct d–d coupling because of full occupation of all spin-up states, while the t_{2g}–t_{2g} repulsion in spin-down channel leads to a net energy gain of $-(3-m_e)\Delta^{t1}_{dd}$ where m_e is the number of electrons in t_2 state. In the AFM configuration, the coupling situations are the same in the spin-up and spin-down channels. From consideration of coupling between the occupied and unoccupied t_{2g} states, the net energy gain is $-(3-m_e)\Delta^{t1,2}_{dd}$. Generally speaking, the magnitude of Δ^{t1}_{dd} is much larger than $\Delta^{t1,2}_{dd}$, leading to the stabilization of FM ordering.

Figure 3 depicts the energy difference between FM and AFM ordering: $\Delta E_{FM-AFM} = E_{FM} - E_{AFM}$ within PBE and HSE03 calculations. We can see that as expected, when the number of additional carrier electrons is less than two per Fe, the AFM magnetic ordering is more stable. This is because the e state captures the adding electrons, while the occupation of the predominating t_2 sates does not change. Thus, the superexchange between t_2 states results in the AFM ground state. Surprisingly, the PBE still gives an AFM ordering ground state when the t_2 becomes partially occupied. This results from the inability of PBE in predicating the correct bandgap of semiconductors. PBE calculations always underestimate the band gap, so that the calculated unoccupied spin-down t_2 state lies above the conductor band minimum (CBM). When the concentration of electron exceeds two per Fe, these electrons first occupy the In 5s band instead of the Fe spin-down t_2 state. The underestimation of bandgap can be overcome by HSE03 functional. The HSE03 is capable of giving the correct band gap and raising the CBM, so the correct position of t_2 states can be obtained. This results in the partial occupation when the number of adding electrons reach 2.5 per Fe. Therefore, the double exchange between minority t_2 states stabilizes the FM order within HSE03 calculations.

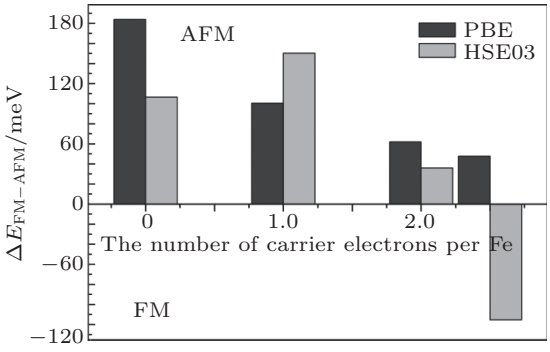


Fig. 3. Energy difference between FM and AFM ordering: $\Delta E_{FM-AFM} = E_{FM} - E_{AFM}$ within PBE and HSE03 calculations.

To verify the theoretical predication that electron-mediated FM in Fe doped InP can be achieved through n-type doping, we have also prepared Fe-doped InP wafer using a diffusion treatment. The temperature-dependent magnetization (M–T) curve for single-phase Fe-doped InP sample is measured using a SQUID magnetometer with a magnetic field of 0.1 T, applied in the direction perpendicular to the film plane. Measurements have also been taken at 0.3 T, and a similar temperature dependence is obtained. The diamagnetic contribution of the InP substrate is subtracted from the results of magnetization. The dc zero-field-cooled (ZFC) and the field-cooled (FC) magnetization curves are shown in Fig. 4. Measurements are performed from 100 to 300 K. The FC is obtained by measuring the magnetic moment of the sample in a magnetic field of 0.1 T during cooling. The ZFC measurement is obtained by first cooling the sample to 5 K in zero fields and then warming it under the same field as that of the FC measurement. The ZFC magnetization shows stronger temperature dependence than the FC one below 200 K. ZFC and FC magnetization curves overlap when the temperature exceeds 300 K, and both exhibit paramagnetic behaviours. Below this temperature, the ZFC–FC curves are separated from each other, and the ferromagnetic behaviour can be seen in Fig. 4. These results indicate irreversibility between the FC and ZFC measurement. At the same time, at 300 K, there still exists a small bifurcation between FC and ZFC, which demonstrates that a net magnetization is still preserved. The AFM ordering is not favourable in this case because AFM has zero net magnetization.

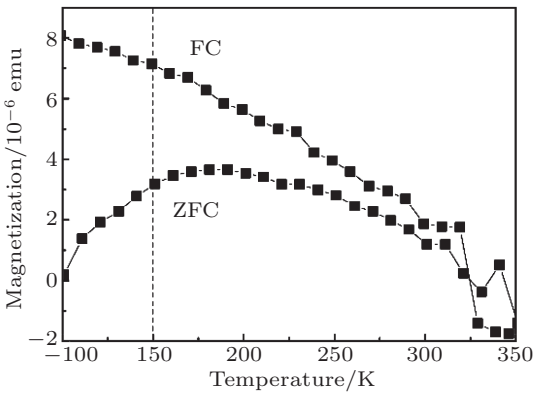


Fig. 4. FC–ZFC M–T curves of the Fe-doped InP sample. The FC is obtained by measuring the magnetic moment while cooling the sample in a magnetic field of 0.1 T and then heating the sample in the same magnetic field. The ZFC is also obtained by measuring the magnetic moment while cooling the sample in the absence of magnetic field and then heating the sample under the same magnetic field as that for FC.

Figure 5 show the hysteresis (M versus H) loop for the n-type doped InP:Fe sample at 150 K. The total magnetization could be described as an algebraic sum of various contributions. The substrate diamagnetic contribution is subtracted from the total magnetization signal. The remaining data consist of the paramagnetic and ferromagnetic contributions from the Fe-doped InP sample. The well-defined hysteresis loop shows that the InP:Fe sample is clearly ferromagnetic at 150 K. At 150 K, the saturation magnetization ($M_{\rm S}$) is 7.66×10^{-6} emu (1 emu=10^{-3} A·m^2) with a remanence magnetization ($M_{\rm R}$) of 1.84×10^{-6} emu and a coercive field ($H_{\rm c}$) of 0.02 T. InP wafer is diamagnetic, so the magnetization data indicate that the ferromagnetization in the present study is caused by Fe-doping in n-type InP bulk material. These experimental results demonstrate the electron-mediated FM in Fe doped InP.

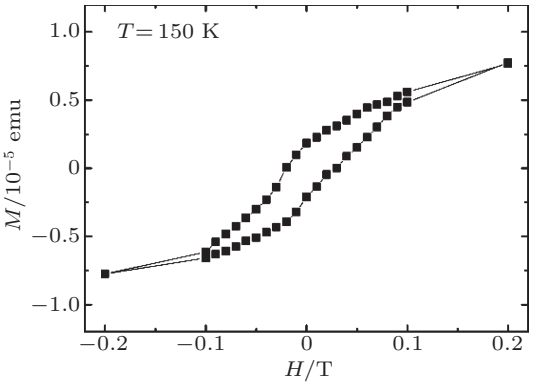


Fig. 5. Curve of M versus H of the sample taken at 150 K after the necessary background diamagnetic subtraction. The magnetic field used ranges from 0 to 0.3 T.

4. Conclusions

In the present paper, the electron-mediated ferromagnetism in Fe-doped InP is confirmed from both first-principles calculations and experiments. Based on spin-polarized density functional theory within HSE03 approach, the magnetic properties of Fe-doped InP are systematically investigated and the existence of electron-mediated ferromagnetism is predicated. The Fe-doped InP showing ferromagnetism is successfully prepared by diffusing Fe into n-type InP wafer, which is consistent with our theoretical predictions.

Acknowledgement

The authors would like to thank Professor Jingbo Li and Dr. Hui-Xiong Deng for their enlightening discussion.

References

[1] Ohno H 1998 *Science* **281** 951

[2] Awschalom D D and Kawakami R K 2000 *Nature* **408** 923

[3] Wolf S A, Awschalom D D, Buhrman R A, Daughton J M, von Molnár S, Roukes M L, Chtchelkanova A Y and Treger D M 2001 *Science* **294** 1488

[4] Linnarsson M, Janzn E, Monemar B, Kleverman M and Thilderkvist A 1997 *Phys. Rev.* B **55** 6938

[5] Fukumura T, Jin Z, Ohtomo A, Koinuma H and Kawasaki M 1999 *Appl. Phys. Lett.* **75** 3366

[6] Jin Z, Fukumura T, Kawasaki M, Ando K, Saito H, Sekiguchi T, Yoo Y Z, Murakami M, Matsumoto Y, Hasegawa T, and Koinuma H 2001 *Appl. Phys. Lett.* **78** 3824

[7] Peng H, Li J, Li S S and Xia J B 2009 *Phys. Rev.* B **79** 092411

[8] Deng H X, Li J, Li S S, Xia J B, Walsh A and Wei S H 2010 *Appl. Phys. Lett.* **96** 162508

[9] Wei S H, Gong X G, Dalpian G M and Wei S H 2005 *Phys. Rev.* B **71** 144409

[10] Dalpian G M, Wei S H, Gong X G, da Silva A J R and Fazzio A 2006 *Solid State Commun.* **138** 353

[11] Peng H, Xiang H J, Wei S H, Li S S, Xia J B and Li J 2009 *Phys. Rev. Lett.* **102** 017201

[12] Dietl T, Ohno H, Matsukura F, Cibert J and Ferrand D 2000 *Science* **287** 1019

[13] Sanvito S, Ordejon P and Hill N A 2001 *Phys. Rev.* B **63** 165206

[14] Coey J M D, Venkatesan M and Fitzgerald C B 2005 *Nat. Mater.* **4** 173

[15] Meng X Q, Tang L M and Li J 2010 *J. Phys. Chem.* C **114** 17596

[16] Walsh A, Da Silva J L F and Wei S H 2008 *Phys. Rev. Lett.* **100** 256401

[17] Wieder H H 1985 *J. Vac. Sci. Technol.* **15** 1498

[18] Petrov M P, Bryksin V V, Hilling B, Lemmer M and Imlau M 2008 *Phys. Rev.* B **78** 085121

[19] Zhu H J, Kostial H, Wassermeier M, Schonherr H P and Ploog K H 2001 *Phys. Rev. Lett.* **87** 016601

[20] Feng Q J, Shen D Z, Zhang J Y, Li B H, Zhang Z Z, Lu Y M and Fan X W 2008 *Mater. Chem. Phys.* **112** 1106

[21] Twardowski A, Swagten H J M and Jonge W J M 1991 *Phys. Rev.* B **44** 2220

[22] Hohenberg P and Kohn W 1994 *Phys. Rev.* B **136** 864

[23] Perdew J P and Wang Y 1986 *Phys. Rev.* B **33** 8800

[24] Perdew J P, Chevary J A, Vosko S H, Jackson K A, Pederson M R, Singh D J and Fiolhais C 1992 *Phys. Rev.* B **46** 6671

[25] Heyd J, Scuseria G E and Ernzerhof M 2003 *J. Chem. Phys.* **118** 8207

[26] Heyd J and Scuseria G E 2004 *J. Chem. Phys.* **120** 7274

[27] Heyd J, Peralta J E, Scuseria G E and Martin R L 2005 *J. Chem. Phys.* **123** 174101

[28] Paier J, Marsman M, Hummer K, Kresse G, Gerber I C and Angyan J G 2006 *J Chem. Phys.* **124** 154709

[29] Kresse G and Hafner J 1993 *Phys. Rev.* B **48** 13115

[30] Monkhorst H J and Pack J D 1976 *Phys. Rev.* B **13** 5188

[31] Madelung O 2004 *Semiconductors: Data Handbook* (Berlin: Springer)